IEEE Access
Multidisciplinary | Rapid Review | Open Access Journal

Received April 10, 2017, accepted May 2, 2017, date of publication May 8, 2017, date of current version June 28, 2017.

Digital Object Identifier 10.1109/ACCESS.2017.2701800

Deep Belief Networks Ensemble for Blood Pressure Estimation

SOOJEONG LEE AND JOON-HYUK CHANG, (Senior Member, IEEE)
Department of Electronic Engineering, Hanyang University, Seoul 133-791, South Korea

Corresponding author: Joon-Hyuk Chang (jchang@hanyang.ac.kr)

This work was supported by the National Research Foundation of Korea under Grant 2016R1D1A1B03932925 and Grant 2014R1A2A1A10049735.

ABSTRACT In this paper, we propose a deep belief network (DBN)–deep neural network (DNN) with mimic features based on the bootstrap inspired technique to learn the complex nonlinear relationship between the mimic feature vectors obtained from the oscillometry signals and the target blood pressures. Unfortunately, we have two problems in utilizing the DBN–DNN technique to estimate the systolic blood pressure (SBP) and diastolic blood pressure (DBP). First, our set of input feature vectors is very small, which is a fatal drawback to training based on the DBN–DNN technique. Second, the special pre-training phase can also trigger an unstable estimation, because there are still a lot of random initialized assigns, such as the training data set, weights, and biases. For these reasons, we employ the bootstrap-inspired technique as a fusion ensemble estimator based on the DBN–DNN-based regression model, which is used to create the mimic features to estimate the SBP and DBP. Our DBN–DNN-based ensemble regression estimator provides a lower standard deviation of error, mean error, and mean absolute error for the SBP and DBP as compared with those of the conventional methods.

INDEX TERMS Blood pressure measurement, oscillometry blood pressure estimation, deep neural networks, bootstrap-inspired technique, ensemble.

I. INTRODUCTION

Blood pressure (BP) is an important vital signal and serves as a core parameter to determine the cardiovascular health of patients [1]–[6]. An oscillometry BP monitor is one of the current standard automatic devices now readily available for the home, office, and hospital. The maximum amplitude algorithm (MAA) based on the oscillometry is generally used to estimate the average of the BP as the cuff pressure at which the maximum oscillation occurs and then linearly relates the SBP and DBP to the mean pressure using empirical coefficients [1], [3]. Thus, these characteristic coefficients are used to determine time points where the cuff pressure corresponds to the SBP on the ascending phase of the oscillometry envelope, while it coincides to the DBP on the descending phase of the oscillometry envelope [3], [4]. However, the characteristic fixed coefficients are not supported by the evidence, because the BPs (SBP and DBP) are consistently changing over time according to intrinsic physiological variabilities such as exercise, stress, food, and environmental factors [4], [5]. As an example, it is found that the BP values provided by patients' monitors differ from those recorded from the auscultatory devices by greater than 5 mmHg approximately 50% and 40% of the measurement for SBP and DBP, respectively [6]. On the basis of the American National Standards Institute and the Association for the Advancement of Medical Instrumentation (ANSI/AAMI) phygmomanometer committee (SP 10) standard, the maximum is limited to the mean error of ± 5 mmHg with a standard deviation 8 mmHg compared with an auscultatory reference reading obtained by at least two trained clinicians [7]. However, the BP can move up to 20 mmHg within a few heartbeats [8]. These variations and their impact on BP measurements are not perceived and accounted for by most physician, which implies BP estimation utilizing available automated devices is subject to two causes of uncertainty. The first cause is a BP measurement device inaccuracy and the second is a physiological variability of the BPs. Even though the uncertainty is introduced by measurement error based on the ANSI/AAMI SP 10 standard, the physiological variability with respect to estimation uncertainty is not addressed [9].

In order to address the problem, alternative techniques such as artificial neural networks (ANNs) [10], [11] have been considered to address the characteristic fixed coefficient problem of the conventional MAA algorithm. These techniques did not use a mathematically or physically complicated models [12], [13] and were suitable only for

nonlinear physiological BP structures [14]. The ANN is more robust with respect to noise and artifact than oscillometric algorithm such as the MAA [1], slope of envelope [1], mathematical models [4] to estimate the BP [10]. Based on these techniques, a two-layer feed-forward neural network (FFNN) based on the back-propagation training algorithm was proposed by Baker [10] to estimate the BP. Also, an approach using the FFNN technique, which consists of two-layer FFNNs with a linear output layer, was performed to compute the gradient using the resilient back-propagation algorithm [14]. Unfortunately, this method is not enough to satisfy the recommendations of the ANSI/AAMI SP10 standard [7]. For these reasons, an intelligent learning-based technique is highly required to estimate the BP accurately without limitations such as the characteristic coefficients and physiological variability.

In this paper, we propose a novel approach using a deep belief network (DBN)-deep neural networks (DNN) based fusion ensemble regression estimator to represent the highly nonlinear relationship between the feature vectors obtained from the oscillometry BP signals and target BPs efficiently [15], [16]. Please note that the DBN proposed by Hinton *et al.* [16] is the superior generative model to learn the complex nonlinear relationship between the explanatory data and dependent variables. Recently, the DBN technique has attracted increasing attention in both the machine learning [17], [18] and signal processing areas as a remarkable technique. The general approach is to employ the DBN-DNN based regression technique to produce a single estimator using a training set [19]. However, it also has some problems. First, it is hard to choose the best DBN-DNN based regression estimator, which is not known during training. The best DBN-DNN-based regression estimator produces the best accuracy as well as good generalization ability for the unseen data. Second, we may throw away valuable information when choosing the DBN-DNN based regression estimator and discarding the others. Third, our input data were a small sample size of only five measurements per subject, which is a fatal drawback while using the DBN-DNN technique [16]. If we have no a *priori* knowledge on the highly nonlinear function, generally speaking, small number of samples may not guarantee successful identification of the DBN-DNN structure of the nonlinear function since there may exist infinite many nonlinear functions fitting the data. This critical weakness can then cause problems such as overfitting because our DBN-DNN based regression model is composed of the complex structures such as many layers, weights, biases, neurons, and nonlinear functions. Given our model, the overfitting problem can be mitigated by the size of our input data increases. Specifically, the DBN was designed to solve overfitting on the training data set using a special pre-training phase. Even though the early stopping and dropout is well known to decrease the overfitting case as simple techniques on the DBN-DNN model, however, we cannot utilize them because they need an appropriate amount of the input data [19]. Interestingly, this pre-training phase in the DBN-DNN based regression model can also trigger an estimation uncertainty, because there are still a lot of random initialized assigns such as the training data set, weights, and biases.

On the basis of these motivations, the DBN-DNN based fusion ensemble regression estimator is proposed to estimate the SBP and DBP without the characteristic coefficients. To address above problems, the bootstrap-aggregation (bagging) [20] and adaboost techniques [21], as a fusion ensemble estimator based on the DBN-DNN based regression model, are used to estimate the SBP and DBP using the small sample. The bagging technique is used for ensemble parameters in the pre-training phase, whereas the adaboost approach is utilized to estimate the SBP and DBP in the fine-tuning phase accurately. In particular, the number of the mimic feature's samples is rapidly increased using the bootstrap-inspired techniques, which generate an ensemble of estimators by training each estimator on a different bootstrap sample of the training set. This work offers an accurate BP estimates without the characteristic coefficients and provides a relevant solution that can decrease the estimation uncertainty. As far as we know, this is one of the first studies applying the DBN-DNN based fusion ensemble regression model for BP estimation with a small training sample. This paper has the following additional improvements and contributions:

- We provide a novel technique to obtain accurate BP estimates from an insufficient sample of oscillometric blood pressure measurements using the DBN-DNN based fusion ensemble regression estimator.
- As a statistical aspect, the DBN-DNN-based regression ensemble estimator can find a superior estimator and mitigate the risk of selecting the wrong estimator [22].
- In a computational viewpoint, we provide a better approximation to the true target BPs than any of the single estimators because of driving the local search from many initial points through the pre-training phase [22].
- For the convergence, the DBN-DNN-based ensemble estimator also minimizes on upper bound on the estimation error [21].
- This method can indeed mitigate the estimation uncertainty such as large the error of standard deviation on comparing the proposed DBN-DNN based ensemble model to the FFNN estimator, we confirm that the SDEs of the SBP and DBP are reduced by 1.87 and 2.11 mmHg, respectively. These imply that the proposed method substantially improve the performance by 24.6% and 31 % compared with the FFNN regression model.
- Our DBN-DNN based ensemble model reduces the SDEs (MAE) of SBP and DBP by 11.0% and 18.1% compared with the DBN-DNN based regression [19].

II. BP ESTIMATION BASED ON ENSEMBLE ESTIMATOR OF DBN-DNN REGRESSION

A. FEATURES OBTAINED FROM OSCILLOMETRY SIGNALS

Filtering and detrending are required to extract the oscillometric signals from the cuff deflation curve. The filtering is to

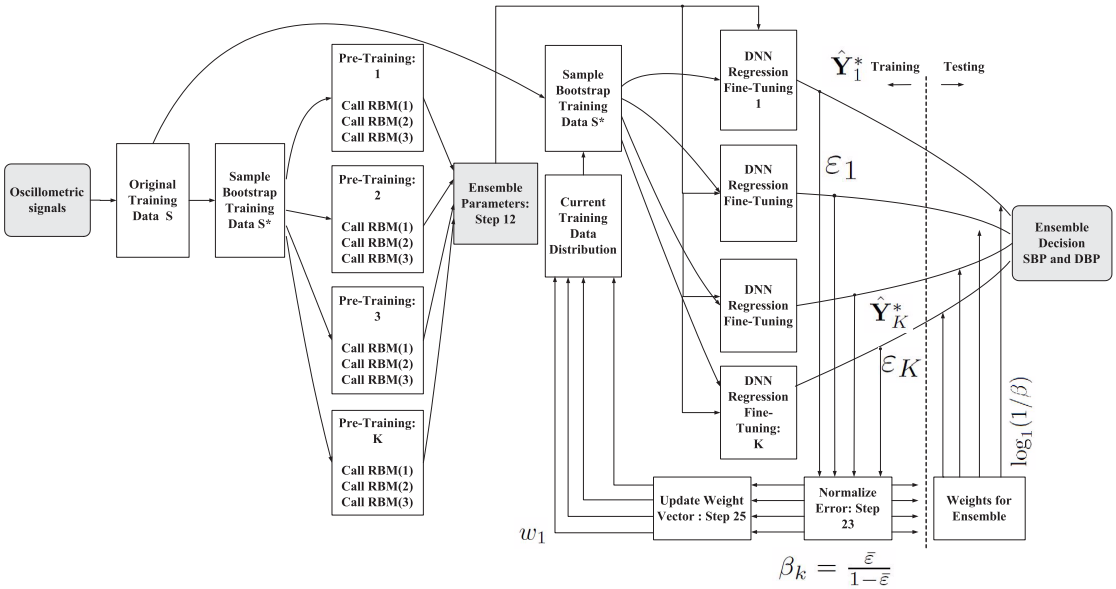

FIGURE 1. A block diagram showing the systolic and diastolic blood pressures estimation using the DBN-DNN based fusion ensemble estimator, where from the step 1 to step 11 denote the DBN structure for the pre-training and the remaining steps are the DNN ensemble estimator.

remove the frequency components that belong to the deflating cuff pressure using a band-pass or high-pass filter [2]. Specifically, the lower cutoff frequency of the filter is generally set to 0.1-0.3 Hz. The detrending is to do a line of best fit that represents the decreasing cuff pressure is subtracted from the cuff deflation curve. After the signal processing of the oscillometry signals such as the noise suppression and smoothing using the weighted median filter, we are then interested in the features obtained from the oscillometry signals [3]. First, we analysis the time and frequency domains of the oscillometry signals. However, there is not effective feature in the frequency domains due to very low frequency around 1-1.5 Hz. Thus, all original features are acquired from the oscillometry signals in the time domain to estimate the reference systolic blood pressure (RSBP) and reference diastolic blood pressure (RDBP) [23], [24], which are used as the target BPs in the proposed DBN-DNN fusion ensemble estimator. We can then use the mean arterial pressure (MAP) estimated using the MAA technique, which is mapped back to the cuff pressure signal [24]. We also utilize the maximum amplitude (MA), the area under the envelope (AE) [23], [24] and the asymmetry ratio (AR) of the oscillometry's envelope [23], [24], which is calculated by dividing the length of the maximum amplitude's position (MAPL) by the length of the envelope (EL) obtained from the oscillometry signals, because this feature represents quite well the characterization of the BPs of individual subjects. The four features from the asymmetrical Gaussian curve function about the oscillometry's envelope are also included, such as the amplitudes, σ_1 and σ_2, which denote the different standard deviations of the asymmetrical Gaussian function [3], [14]. We also add the average of the oscillometry signal's heart rate, the oscillometry signal's maximum positive of temporal rate change of amplitude [24], the subject's age, and the subject's gender [24]. Thus, eleven feature vectors are collected to estimate the target BPs (RSBP and RDBP). A common normalization technique is then utilized to restrict the ranges of the allowed feature values to lie between the minima and maxima of the predefined ranges [24].

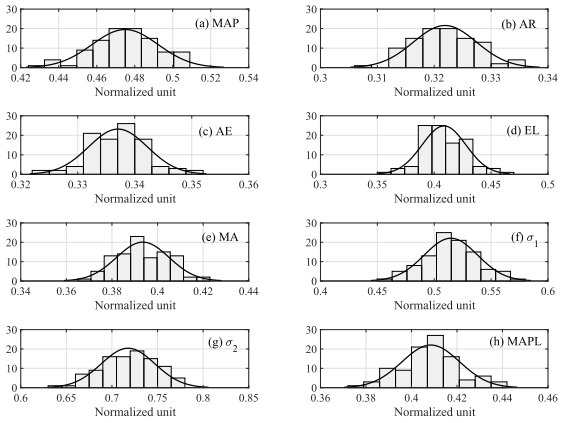

FIGURE 2. The plots of distribution of artificial features based on the parametric bootstrap approach with replication numbers (B=100). Note that these artificial figures are examples obtained from one subject with 5 samples for 8 features [19].

From the above mimic feature distribution, the normality of each mimic feature distribution is validated as shown in Fig. 2. Specifically, we utilize the Kolmogorov-Smirmov (KS) test [25], which is commonly known as the statistical test, where the distribution of these mimic feature

fits the Gaussian distribution quite well. Suppose that we obtain F_* a distribution of mimic feature $\{x_1^*, x_2^*, \ldots, x_B^*\}$ from unknown sample distribution F. Thus, it is required to test the hypothesis that F_* becomes to the Gaussian distribution F_0. The null hypothesis states that the observed blood pressure measurement has an approximately Gaussian distribution. The alternative hypothesis describes that the observed blood pressure measurements does not approximately resemble a normal. H_0: there is no difference between the observed measurements of BP and a normality distributed empirical measurements. Meanwhile, H_1: there is a difference between the observed measurements of BP and a normality distributed empirical measurements. Moreover, we confirm that the test results of all mimic features are 0. Thus, we cannot reject the null hypothesis states at the 0.05 significant level. Also, the all p values of the KS test are greater than the level of the 0.05 significant level. Additionally, if KS values are greater than the critical values, the null hypothesis is rejected. Therefore, we do not reject the null hypothesis states for that the observed measurements are sufficiently normal. Thus, the mimic features have very similar statistical characteristic as the original feature vectors. The remaining features also denote similar results. Thus, the distribution of the mimic features acquired using the parametric bootstrap are represented in Fig. 2 (B=100). As the number of replication B gets large, the distribution becomes more closely the Gaussian distribution [3].

B. DBN-DNN ENSEMBLE REGRESSION

One of the core advantages of the DBN-DNNs regression model is its powerful generalizability over the conventional FFNN technique [15]. Specifically, an unsupervised learning technique initializes a good set of parameters because the unsupervised training makes it easier to optimize many parameters before overfitting occurs, which is called pre-training technique [16]. After pre-training phase, a supervised learning step is performed through the back-propagation algorithm to fine-tune the parameters obtained from the pre-training phase [15], [16]. The pre-training step makes it possible to find abstractions from the lowest level features to highest level concepts. Namely, the input features are to be mapped into gradually higher levels of representation through the deep architectures [26].

The mimic feature is generated by the bootstrap-inspired technique to improve the performance of the estimates from a small number of measurements in situations where improving the performance of conventional methods is not a valid approach [3]. Considering the proposed DBN-DNN regression model, the target function can be defined as $\mathbb{E}[Y|X]$. In this work, suppose $X = \{x_1, \ldots, x_N\}$ and $Y = \{y_1, \ldots, y_N\}$ are random samples of the distribution $\mathbb{F}$ with unknown parameters $\{\mu, \sigma\}$, respectively. Thus, we can only apply the estimated distribution $\hat{\mathbb{F}}$ by using sample parameters $(\hat{\mu}, \hat{\sigma}|X)$, where the mean and standard deviation are given by $\mathbb{E}(\mu|X) \simeq \hat{\mu} = \bar{x} = \frac{1}{n}\sum_{i=1}^{n} x_i$ and $\mathbb{E}(\sigma|X) \simeq \hat{\sigma} = \sqrt{\frac{1}{n-1}\sum_{i=1}^{n}(x_i - \bar{x})^2}$, where $\hat{\mathbb{F}} \simeq \mathcal{N}(\hat{\mu}, \hat{\sigma}^2)$ is approximated as a Gaussian distribution $\mathcal{N}(\mu, \sigma^2)$, which is called the parametric bootstrap [27]. The parametric bootstrap is used to generate the mimic features obtained from the original feature vectors which have *a priori* information such as the mean and standard deviation for each subject; this is different from the original bagging method [20], because this is used to estimate $\mathbb{F}$ without any *a priori* assumptions, which is called the nonparametric bootstrap technique [27]. Specifically, instead of sampling with replacement from $X = \{x_1, \ldots, x_N\}$, we generate B samples X_b^* with size $N = 5$ and $\forall b \in \{1, \ldots, B\}$ from $\mathbb{F}_{\hat{\mu},\hat{\sigma}}$, as shown in Table 1, where N denotes the number of BP measurement data point for each subject. On the parametric technique, even though the oscillometry may be a time series with autocorrelation and dynamics, the mimic feature vectors $\mathbf{X}_i^* = \{\bar{X}_{i,1}^*, \bar{X}_{i,2}^*, \ldots, \bar{X}_{i,B}^*\}$ can be finally calculated as given in steps (7)-(9). In step (7), $X_{i,b}^* = \{x_1^*, x_2^*, \ldots, x_N^*\}$ as bootstrap replication data are generated from the original feature vector $X = \{x_1, \ldots, x_N\}$, which exactly corresponds to the mimic feature vectors using the moving block bootstrap because the bootstrap samples based on $\mathbb{F}_{\hat{\mu},\hat{\sigma}}$ are calculated using the Monte-Carlo method [27] as shown in Table 1. The moving block bootstrap is an ideal technique on the nonparametric bootstrap technique because given $N = 5$, we can randomly select block k from the original feature vector $X = \{x_1, \ldots, x_N\}$ and connect together to make a resample with respect to the time series [27]. A similar procedure is used to create the mimic features from $Y = \{y_1, \ldots, y_N\}$ in order to be used as the target vectors. Thus, the sufficient feature samples are ready to estimate the target BPs (RSBP and RDBP) efficiently as training data sets, whereas the unseen feature vectors are used as the test data. As shown in the steps of Table 1.

We firstly propose a fusion ensemble approach combining as the bagging and adaboost [20], [21] techniques to address the problem of small samples for each subject and the unstable performance of the DBN-DNN regression estimator. In this section, we explain how ensemble fusion using the bagging and adaboost techniques can be used for the DBN-DNN regression estimator, as shown in Table 1. There are two phases: the upper phase represents the pre-training phase, whereas the lower phase expresses the fine-tuning. The upper phase starts with the input features obtained from the oscillometry signals. First, we can define our input features as $S = \{X_i, Y_i\}$, where X_i denotes the explanatory vector and Y_i are the response vectors, as shown in step (2). Each feature vector is used to compute the parameters such as the mean μ and standard deviation σ. We then initialize a weight vector $w_m^{(1)}$ to be used in the fine-tuning. Then, the parametric bootstrap function is called to generate the bootstrap resampled distribution, as shown in steps (7)-(9). Next, we also call the RBM [16] function to mitigate the overfitting and local minima problems. However, this phase in the DBN-DNN based regression estimator may also trigger an unstable estimation, because there are many random initialized assigns such as the training data set, weights, and biases. Thus, we need to address this problem through the ensemble process, as

TABLE 1. The algorithm is an example of mimic feature creation using the ensemble estimator based on the parametric bootstrap-inspired technique for each subject, where *I* denotes the number of input feature (MAP, AR,...), *J* is the number of target BPs (SBP and DBP), and B represents the number of parametric bootstrap replication.

Algorithm	(Ensemble algorithm with DBN-DNN)
step 1:	oscillometric signals
step 2:	input feature vectors: $X_i = \{x_1, x_2, ..., x_N\}$ and $Y_j = \{y_1, y_2\}$, $\forall i = 1$ to I *(=11)* and $\forall j = 1$ to J *(=2)*, explanatory matrix: $\mathbf{X} = \{X_1, X_2, ..., X_I\}$ and response (targets) matrix: $\mathbf{Y} = \{Y_1, Y_2\}$, $\mathbf{S} = \{\mathbf{X}, \mathbf{Y}\}$
step 3:	calculate parameters: $\mathbb{E}(\mu, \sigma \vert X_i)$ and $\mathbb{E}(\mu, \sigma \vert Y_j)$,
step 4:	initialize weight vector $w_m^1 = 1/M$
step 5:	**for** $k = 1 : K$ do
step 6:	**for** $b = 1 : B$ do
step 7:	call parametric bootstrap replication: $X_{i,b}^* = \{x_1^*, x_2^*, ..., x_N^*\}$ and $Y_{j,b}^* = \{y_1^*, y_2^*, ..., y_N^*\}$, $\forall b = 1$ to B,
step 8:	calculate average: $\bar{X}_{i,b}^* = \frac{1}{N}\sum_{n=1}^{N} x_n^*$ and $\bar{Y}_{j,b}^* = \frac{1}{N}\sum_{n=1}^{N} y_n^*$
step 9:	generate mimic feature: $\mathbf{X}_i^* = \{\bar{X}_{i,1}^*, \bar{X}_{i,2}^*, ..., \bar{X}_{i,B}^*\}$ and $\mathbf{Y}_j^* = \{\bar{Y}_{j,1}^*, \bar{Y}_{j,2}^*, ..., \bar{Y}_{j,B}^*\}$
step 10:	call pre-training phase: $\mathbf{RBM}^1$ $\{\hat{f}^{*k}(\mathbf{X}_i^*)\}$, $\mathbf{RBM}^2$ $\{\hat{f}^{*k}(\mathbf{X}_i^*)\}$, $\mathbf{RBM}^3$ $\{\hat{f}^{*k}(\mathbf{X}_i^*)\}$
step 11:	**end**(b), where b denotes the index of parametric bootstrap replication. **end**(k), where k is the index of estimator
step 12:	ensemble estimator: $\hat{f}_{\varphi}(\cdot) = K^{-1}\sum_{k=1}^{K}(\hat{f}^{*k}(\mathbf{X}_i^*))$ output: parameters (weights and biases) for fine tuning
step 13:	call back-propagation phase:
step 14:	**for** $k = 1 : K$ do
step 15:	**for** $b = 1 : B$ do
step 16:	call parametric bootstrap replication: $X_{i,b}^* = \{x_1^*, x_2^*, ..., x_N^*\}$ and $Y_{j,b}^* = \{y_1^*, y_2^*, ..., y_N^*\}$, $\forall b = 1$ to B,
step 17:	calculate average: $\bar{X}_{i,b}^* = \frac{1}{N}\sum_{n=1}^{N} x_n^*$ and $\bar{Y}_{j,b}^* = \frac{1}{N}\sum_{n=1}^{N} y_n^*$
step 18:	generate mimic feature: $\mathbf{X}_i^* = \{\bar{X}_{i,1}^*, \bar{X}_{i,2}^*, ..., \bar{X}_{i,B}^*\}$ and $\mathbf{Y}_j^* = \{\bar{Y}_{j,1}^*, \bar{Y}_{j,2}^*, ..., \bar{Y}_{j,B}^*\}$, $\forall i = 1$ to I *(=11)* and $\forall j = 1$ to J *(=2)*
step 19:	weighted sample M from sequence of L, $\mathbf{S}^* = \{\mathbf{X}^*, \mathbf{Y}^*\}$ using weights $w_m^{(k)}$ with replacement $(M \leq L)$, where L denotes the number of the whole mimic sample ($L = B \times S$(the subject number))
step 20:	call learning: **back-propagation** $\{\hat{f}^{*k}(\mathbf{X}_m^*, \mathbf{Y}_m^*)\}$, output: $\hat{\mathbf{Y}}_m$, $\forall m = 1$ to M
step 21:	$\varepsilon_m = \frac{[\hat{\mathbf{Y}}_m - \mathbf{Y}_m^*]^2}{\varepsilon_{\max}}$, where $\varepsilon_{\max} = \max_{m=1,...,M}[\hat{\mathbf{Y}}_m - \mathbf{Y}_m^*]^2$
step 22:	$\bar{\varepsilon} = \sum_{m=1}^{M} \varepsilon_m w_m^{(k)}$
step 23:	$\beta_k = \frac{\bar{\varepsilon}}{1-\bar{\varepsilon}}$
step 24:	$w_m^{(k+1)} = w_m^{(k)} \beta_k^{(1-\varepsilon_m)}$
step 25:	$w_m^{(k+1)} = \frac{w_m^{(k+1)}}{\sum_m w_m^{(k+1)}}$
step 26:	**end**(b), where b denotes the index of parametric bootstrap replication. **end**(k), where k is the index of estimator

shown in step (12). Therefore, the average parameters such as the weights and biases that are obtained through the bagging technique are used for the fine-tuning phase. Otherwise, the adaboost technique of the lower phase adaptively adjusts the distribution of the original training set before each new bootstrap sample is obtained. For each estimator, it then generates a different training set by sampling with replacement from the bootstrap training set according to the weighted training samples, as expressed in step (19). Specifically, the bootstrap samples are obtained from a distribution that is iteratively updated by a relative error function for the subsequent estimator. The weight of each instance is adjusted in accordance with its difficulty, i.e., the previously large incorrect instances are more likely to appear in the next bootstrap sample. Accordingly, the adaboost technique will thus lead to decrease the variance of the mean error and increase the confidence of the results for the DBN-DNN regression estimator. As shown in step (20), the back-propagation is called to estimate the target BPs. We then recursively compute the error between the estimated ($\hat{\mathbf{Y}}^*$) and target BPs ($\mathbf{Y}$) until the minima of the errors are found, as shown in step (21). The average error is calculated as expressed in step (22), and then the weight updating parameter β_k is given as in step (23). Finally, we update the weight vector for elements and normalize as shown in steps (24)-(25). If an element in the current iteration has a large error, β_k will be large, whereas if the error of the element is very small, the weight will be reduced. Therefore, the final output of the fusion ensemble estimator is given as

$$\hat{\mathbf{Y}}^* = \inf\left\{y \in \mathbf{Y} : \sum_{k:\hat{y}_k \leq y} \log(1/\beta_k) \geq 0.5 \sum_{k} \log(1/\beta_k)\right\}. \tag{1}$$

Here, each of the K estimator makes a prediction $\hat{y}_k$, $\forall k = 1$ to K. Summing up the $\log(1/\beta_k)$ until we reach the smallest

k so that the inequality is satisfied. If the β_k are all equal, it would be the median value. For details on the theorem of ensemble estimator, the reader is referred to [21]. The following theorem represents the guarantee of our ensemble estimator [21].

TABLE 2. Parameter setting [15], [16], [26] of the DBN-DNN based fusion ensemble regression model, where 11 is the number of input units (namely, the input vector's dimension) and 2 denotes the number of output units (namely, the target vector's [SBP and DBP] dimensions).

Number of the hidden unit in three layers:	$[(11,(32),(32),(32),2)]$
Number of feature vector (X)	11
Number of target vector (Y)	2
Number of sample over each mimic feature	100
Number of sample over each original feature	5
Number of hidden layers	3
Number of hidden unit on the layers	16 to 256
Number of ensemble	50
Learning rate for weight	0.001
Learning rate for biases of visible units	0.01
Learning rate for biases of hidden units	0.01
Momentum rate	0.9
Activation type	sigmoid type function
Maximum epoch in the pre-training	200
Maximum epoch in the fine-tuning	200
Initial weights and biases	randomly between (-1, 1)

Theorem: Suppose the DBN-DNN algorithm, when called by the adaboost technique for the regression model, generates hypotheses with errors $\{\varepsilon_1, \varepsilon_2, \ldots, \varepsilon_K\}$, where ε_k is as defined in Table 2. Then, the mean square error $\varepsilon = \mathbb{E}[(\hat{\mathbf{Y}}^* - \mathbf{Y})^2]$ of the final output of the hypothesis by the adaboost technique is bounded above by

$$\varepsilon \leq 2^K \prod_{k=1}^{K} \sqrt{\varepsilon_k(1-\varepsilon_k)} \tag{2}$$

On the basis of this theorem and proof about the adaboost algorithm [21], the DBN-DNN based fusion ensemble regression estimator can be used as a stable estimator. The DBN-DNN based fusion ensemble regression can then be defined as

$$\hat{f}_{\varphi}^{*}(\cdot) = \mathcal{D}_{NN}((\mathbf{X}^*, \mathbf{Y}^*))(\cdot) : \mathbb{R}^I \rightarrow \mathbb{R}^J$$

where $\mathcal{D}_{NN}(\cdot)$ denotes the estimator based on the DBN-DNN regression model that will be represented as follows.

C. DESIGN OF DBN-DNN REGRESSION ESTIMATOR

The DBN-DNN regression estimator has two training steps, a greedy layer-wise unsupervised pre-training (DBN) at each layer to preserve information from the input data and a supervised fine-tuning (DNN) of the whole DBN-DNN in terms of the ultimate target estimation [16], [28], where the DBN denotes a top-down model calculated from the hidden layer to input data. The DNN is a bottom-up propagation from input data to the top layer based on a non-probability model. One the other hand, the DBN is probabilistic generative model [16] that comprises multi-hidden layers of stochastic variables, where top two layers denote undirected connections, which has defined as

$$P(\mathbf{X}^*, \mathbf{h}^1, \mathbf{h}^2, \ldots, \mathbf{h}^l) = \left(\prod_{i=1}^{l-2} P(\mathbf{h}^i|\mathbf{h}^{i+1})\right) P(\mathbf{h}^{l-1}, \mathbf{h}^l) \tag{3}$$

where the probabilities of the condition layers $P(\mathbf{h}^i|\mathbf{h}^{i+1})$ are factorized conditional distributions [26], $\mathbf{h}^i$ denote the hidden units at layer i and $\mathbf{X}^*$ is the resampled input vector. Note that we will omit the subscripts i and j in the previous section as $\mathbf{X}^* = \mathbf{X}_i^*, \forall i$ in Table 1 to avoid confusing the subscripts between the subsections. The hidden layer $\mathbf{h}^i$ is a binary random vector with $\mathbf{h}_j^i$. In particular, the top-level *a priori* probability $P(\mathbf{h}^{l-1}, \mathbf{h}^l)$ represents a restricted Boltzmann machines (RBM) [16] between the layers. Specifically, our DBN-DNN regression model is a deep generative model that mimics target BPs (SBP and DBP) by stacking multiple restricted Boltzmann machines (RBMs) [16]. An RBM is made up of a two-layer, bipartite, generative undirected model with a set of binary hidden units $\mathbf{h}$ and a set of visible units $\mathbf{X}^*$ in our case. Also, a weight matrix $\mathbf{W}$ ties the visible units and the hidden units [15]. Each hidden unit uses the hyperbolic tangent function to be activated, and the type of the output is used as the linear value. In this work, the Gaussian-Bernoulli RBM [16] is used to connect the Gaussian visible layer and binary hidden layer, because our mimic feature vectors are asymptotically Gaussian distribution. The several Bernoulli-Bernoulli RBMs are then stacked behind the first Gaussian-Bernoulli RBM [16]. The contrastive divergence as a faster learning procedure is used to train the first Gaussian-Bernoulli RBM [16], [26] as an unsupervised learning to minimize the negative log probability of the training vectors. Then, the second Bernoulli-Bernoulli RBM is trained using the information of the first Gaussian-Bernoulli RBM's hidden layer as the second RBMs visible layer [16]. Generally, the DNN is trained by the back-propagation algorithm [26]; however, this is often leads to poor local optima due to the randomly initialized parameters. The weights and biases are thus initialized by pre-training [26] to overcome the poor local optimum problem in the training stage. Unfortunately, random guessing may also use to address this by adopting the pre-training values as the initial weights and biases, because the randomly initialized parameters in the pre-training can cause unstable estimation in the fine-tuning stage. To suppress this problem, we employ the bagging technique for the weights and biases between the RBMs, as shown in Table 1. The DBN-DNN based ensemble regression estimator technique will help to address the problem of instability due to the small sample size. After the pre-training with the ensemble technique, the multiple RBMs can be used as an effective starting point via the ensemble weights and biases for fine-tuning by back-propagation [16]. Therefore, the cost function uses the minimum mean square error (MMSE) criterion [28], [29] using a mini-batch scaled conjugate gradient function between the estimated BP and auscultatory

BP defined as

$$\begin{aligned}\mathbb{E}(\| \widehat{\mathbf{Y}}^* - \mathbf{Y} \|^2) &= \int \| \widehat{\mathbf{Y}}^* - \mathbf{Y} \|^2 P^{\mathbf{Y}}(\mathbf{Y}) d\mathbf{Y} \\ &= \min \mathbb{E}(\| \widehat{\mathbf{Y}}^* - \mathbf{Y} \|^2) \\ &= \frac{1}{N} \sum_{m=1}^{N} \sum_{d=1}^{D} \left[\widehat{\mathbf{Y}}_m^{*d}(\mathbf{W}) - \mathbf{Y}_m^d \right]^2 \end{aligned} \quad (4)$$

where $\widehat{\mathbf{Y}}^*$ and $\mathbf{Y}$ are the estimated and auscultatory BP vectors at the sample index m, N and D represents the mini-batch size and the feature vector's size, $\mathbf{W}$ represent the weights and bias parameters which are learned at the i^{th} layer. The estimated weights and bias can then be updated iteratively as follows:

$$\mathbf{W}_{m+1}^i = -\varepsilon \frac{\partial \mathbb{E}(\| \widehat{\mathbf{Y}}^* - \mathbf{Y} \|^2)}{\partial (\mathbf{W}_m^i)} + \eta(\mathbf{W}_m^i), \quad 1 \le i \le L+1 \quad (5)$$

where ε denotes the learning rate, η is the momentum parameter, L is the number of hidden layers, and $L+1$ denotes the output layer. We can thus obtain $(\hat{\mathbf{Y}}_1^*, \hat{\mathbf{Y}}_2^*, \ldots, \hat{\mathbf{Y}}_K^*)$ as expressed in steps (19)-(24) in Table 1. Finally, we can estimate the target BP $\mathbb{E}^*[\mathbf{Y}] = \bar{\mathbf{Y}}^*$ as given in Eq. (1). As a whole, our DBN-DNN based fusion ensemble estimator is used to learn the complex mapping between the mimic feature vectors and target BPs, and it can adaptively learn the complicated relationship to estimate the target BPs (RSBP and RDBP) from the mimic feature vectors given plenty of training samples by using the bootstrap-inspired fusion ensemble technique [27] in the DBN-DNN training stage. Finally, the SBP and DBP in our DNN estimation stage are stably estimated with assistance of the many DNN ensemble fusion estimators. The primary advantage of using ensemble fusion estimators is the ability to decrease the variance and increase the confidence in determining the SBP and DBP.

III. EXPERIMENTAL RESULTS

This study was conformed by a research ethics committee, and every participant signed informed consent prior to measurement, according to the BP measurement protocol of the institutional research ethics board. The BP measurements were measured from 85 healthy subjects with no history of cardiovascular disease, aged 12 to 80 years, of which 37 were females and 48 were males. Five sets of BP measurements from each subject (duration range of a single measurement: 31-95 sec., duration median: 55 sec.) were acquired utilizing a wrist-worn blood pressure device at a sampling rate of 100 Hz according to the recommendations of the ANSI/AAMI SP 10 standard [7], [24]. Specifically, the readings of two independent nurses were averaged to offer one SBP and one DBP reading [3]. Our BP measurements were comprised of an oscillometric BP recording led by two trained nurses following one minute of rest. This process was repeated four more times to build a recording of five BP measurements. Each participant comfortably sat upright in a chair in which the device cuff was strapped to the left wrist of the subject and raised to heart level during data collection. The auscultatory cuff, that was the reference device, was placed on the upper left arm, also at heart level. The upper cuff was inflated around the arm in order to occlude the brachial artery. When the cuff signal deflated, blood flow generated Korotkoff sounds, that could be readily heard through a stethoscope placed next to the upper cuff. The first Korotkoff sound (K1), that was measured in mmHg by a manometer of the upper cuff, was utilized to estimate SBP, whereas the fifth sound (K5) was used to estimate DBP [30]. Concurrent brachial and wrist measurements were not possible because of the difficulty of occlusion of brachial arteries by upper arm sphygmomanometers. Thus, almost 1.5 min after each signal was obtained by the monitor of the wrist measurement, two trained nurses concurrently recorded systolic blood pressure (SBP_1 and SBP_2) and diastolic blood pressure (DBP_1 and DBP_2) using a classic upper arm sphygmomanometer. Therefore, the mean values of concurrent readings was utilized as the reference BPs (SBP and DBP). Readings with subscript 1 were obtained by the first nurse, and readings with subscript 2 were obtained by the second nurse. The BP measurements of the five sets are given by $\{SBP_{1,j}, SBP_{2,j}, |j = 1, \ldots, 5\}$ and $\{DBP_{1,j}, DBP_{2,j}, |j = 1, \ldots, 5\}$ for each participant, respectively. For details on BP measurements collection, the reader is referred to [24].

Based on the experimental conditions, we performed the training and test experiments to verify the proposed DBN-DNN based fusion ensemble regression estimator. In the proposed scenario, the measurements of subjects were sequentially separated into the training set (250 measurements obtained from 50 subjects with five measurements each) and the testing set (175 measurements obtained from 35 subjects with five measurements each). This process was then repeated such that each subject was included once in the testing stage. Testing in the proposed test scenario may look like examining the generalizing ability of the proposed approach with measurements from new subjects. Indeed, five measurements (i.e., 5 samples over each feature) from each subject is an extremely small number as input data in the training stage. Therefore, we used the mimic features obtained from the original feature vectors. Note that in the test stage, we utilized the unseen original feature set to verify the proposed algorithm. As mentioned, our feature vectors were obtained from the oscillometry signals, which were used to create the mimic feature vectors using the bootstrap-inspired technique [27] for the DBN-DNN based fusion ensemble regression estimator. We thus could obtain the mimic feature vectors with (B=100) training samples over each feature, which implies that each subject has (B=100) training samples over each feature.

In Table 2 shows the configuration and parameter settings of our DNN-based fusion ensemble technique. Specifically, the number of feature vectors (11) represents the features such as the MAP and AE, while the number of samples over each mimic feature (100) was obtained using the bootstrap-inspired technique, as described in section II (b). Based on these configuration, we tested the performance of the

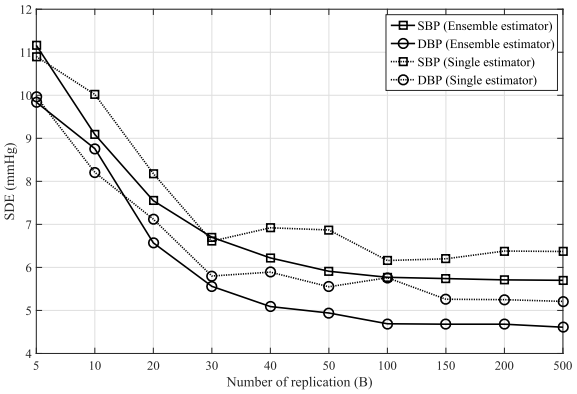

FIGURE 3. Summary of the SDE (ME) obtained using the proposed DBN-DNN based fusion ensemble regression estimator vs. DBN-DNN based single regression estimator as the number of training sample increases based on the AAMI standard protocol, where B is the number of replication about the mimic feature vectors with (from B=5 to 500) training samples for each subject, which implies that each feature has (from B=5 to 500) training samples. As a result, we obtained 25000 input vectors (i.e., 50 subject × B, in case of $B = 500$) over each feature in the training stage.

TABLE 3. Comparison of the complexity of in terms of running time [32], where the specifications of system are Intel® Core(TM) i7-4790 CPU 3.60 GHz, RAM 32.0 GB, OS 64 bit, and Matlab® 2015 (The MathWorks Inc., Natick, Ma, USA).

Method	DBN-DNN	DBN-DNN ensemble
Total time (s)	327.118	13407.286

proposed algorithm based on the same conditions with different number of hidden units from 16 to 256. The best result of the proposed approach was obtained at 64 hidden units, which indicated that a small number of hidden units can lead to an increase in the mean absolute error (MAE) and standard deviation of error (SDE) [31] owing to underfitting, whereas a larger number of hidden units can increase the MAE and SDE due to overfitting. We also conducted another test to prove the performance of the proposed algorithm based on the same conditions with the number of bootstrap replications varying (B) from 5 to 500 for the mimic features. Fortunately, we found that the proposed algorithm had fairly good results as the number of replications changed. We found that the proposed DBN-DNN based fusion ensemble estimator gave more reliable results compared to the DBN-DNN based single estimator as shown in Fig. 3. This demonstrates that the estimation uncertainties were efficiently reduced as shown the solid lines for the SBP and DBP in Fig. 3. In order to compare the computational running time between the DBN-DNN based single estimator and proposed algorithm, we set the number of hidden unit and the number of epoch as 32 and 100. The remaining parameter values were set as in Table 2. Note that the running time is eventually computed based on the performance in Matlab® 2015 [32]. The result noticed that the proposed algorithm did give much higher computation time (s) compared to the DBN-DNN based single estimator, which is mainly due to the ensemble step. Thus, we need to reduce the running time as shown in Table 3.

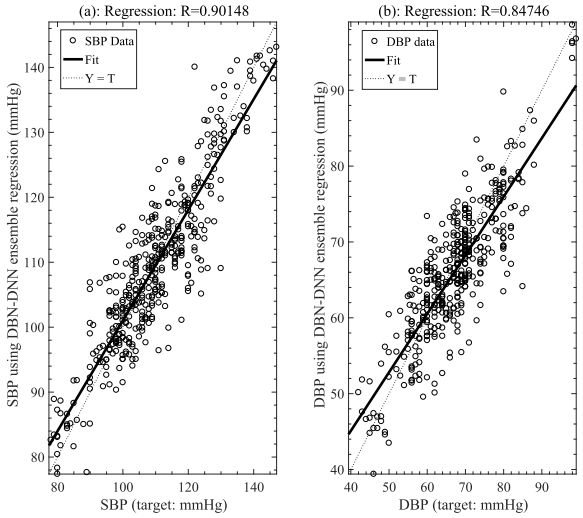

FIGURE 4. Panel (a) shows scatter plot for regression model estimation between the referenced auscultatory SBP and the estimated SBP using the proposed DBN-DNN based fusion ensemble regression estimator and panel (b) denotes scatter plot for regression model estimation between the referenced auscultatory DBP and the estimated DBP using the proposed DBN-DNN based fusion ensemble regression estimator.

To evaluate the proposed technique, we first investigated the degree of similarity between the readings measured with the proposed DBN-DNN based fusion ensemble regression estimator and those measured with the auscultatory method as shown Tables 4 and 5. The proposed method have effect on the SEEs, compared to the MAA because DBN-DNN based fusion ensemble regression have lower SEEs (5.93 mmHg in the SBP and 5.10 mmHg in the DBP), compared with the MAA (8.83 mmHg in the SBP and 6.62 mmHg in the DBP), compared to with the DBN regression (6.45 mmHg in the SBP and 5.24 mmHg in the DBP). These imply that the proposed method represents 32.8% in the SBP and 23% reduction effect compared with the conventional MAA and shows 8.1% in the SBP and 2.7% reduction effect compared with the DBN-DNN regression. As shown Fig. 4 and Table 5, the Pearson correlations (0.901 in the SBP and 0.847 in the DBP) between the DBN-DNN based fusion ensemble regression model and the auscultatory method were compared with those (0.882 in the SBP and 0.838 in the DBP) between the DBN-DNN single regression and the auscultatory method. Those may be noted that the proposed ensemble regression model had the highest the degree of similarity than the conventional methods including the DBN-DNN regression, compared with the auscultatory method.

We also confirmed the mean error (ME) and the SDE between the estimated BPs $\hat{t}_i, i = 1, 2, \ldots, n$ and the reference BPs $(t_i, i = 1, 2, \ldots, n)$ according to the recommendations of the AAMI standard protocol [7] to verify the overall performance of the proposed fusion ensemble algorithm. A BP measurement device can pass the AAMI protocol if the ME is less than 5 mmHg with an SDE of no more than 8 mmHg [7]. Thus, the lower values of the ME and SDE represent the better overall result. However, the

TABLE 4. Summary of the BP measurements using the MAA, FFNN, SVR, GMR, DBN-DNN and the proposed DBN-DNN with ensemble, where SEE denotes standard error of estimate.

BP (mmHg)	SEE (Nurse vs. MAA)	SEE (Nurse vs. FFNN)	SEE (Nurse vs. SVR)	SEE (Nurse vs. GMR)	SEE (Nurse vs. DBN-DNN)	SEE (Nurse vs. DBN-DNN ensemble)
SBP	8.83	7.34	7.14	7.12	6.45	5.93
DBP	6.62	6.01	5.26	5.25	5.24	5.08

TABLE 5. Summary of the BP measurements using the MAA, FFNN, SVR, GMR, DBN-DNN and the proposed DBN-DNN with ensemble, where R is correlation value.

BP (mmHg)	R (Nurse vs. MAA)	R (Nurse vs. FFNN)	R (Nurse vs. SVR)	R (Nurse vs. GMR)	R (Nurse vs. DBN-DNN)	R (Nurse vs. DBN-DNN ensemble)
SBP	0.775	0.832	0.853	0.855	0.882	0.901
DBP	0.736	0.810	0.840	0.842	0.838	0.847

TABLE 6. ME and SDE relative to the reference auscultatory method obtained with the conventional MAA, FFNN, SVR [33], GMR, DBN-DNN based single regression model (DBN-DNN) [19], and using the proposed DBN-DNN based fusion ensemble regression estimator (DBN-DNN ensemble) in the text, where the results are the average values for our test data.

mmHg	MAA		FFNN		SVR		GMR		DBN-DNN		DBN-DNN ensemble	
Test	SBP	DBP	SBP	DBP	SBP	DBP	SBP	DBP	SBP	DBP	SBP	DBP
ME	1.07	1.12	-0.30	0.01	-0.20	0.15	1.35	0.62	0.01	0.22	-0.01	-0.04
SDE(ME)	9.03	7.40	7.61	6.79	7.11	6.14	7.02	6.08	6.20	5.26	5.74	4.68
RMSE	8.42	7.68	6.42	5.93	6.30	5.82	6.12	5.29	4.39	3.94	3.95	3.36
SDE(RMSE)	9.75	9.40	8.55	7.25	8.52	7.19	5.75	4.92	5.10	4.35	4.54	3.53

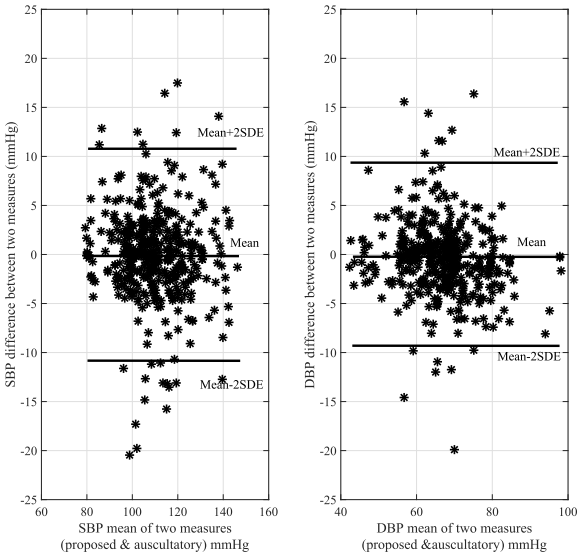

FIGURE 5. The Bland-Altman plots comparing the performance between the proposed DBN-DNN based fusion ensemble regression estimator and the auscultatory nurse measurements [7]. (a) Bland-Altman plot for the SBP. (b) Bland-Altman plot for the DBP.

SDE is more important than the ME, because a BP measurement device can be very inaccurate, and the BP measurements can have small ME values with large errors, which are equally probable to be positive or negative. The MEs of the SBP and DBP acquired using the proposed DBN-DNN based ensemble regression estimator were compared to those of the MAA [24], FFNN [14], support vector regression (SVR) [33], GMR [23], DBN-DNN single model [19], and DBN-DNN based regression ensemble model as shown in Table 6. Note that the mimic features were fairly used in the opponent algorithms except for the MAA [24]. From Table 6, the SDE values obtained by our DBN-DNN based fusion ensemble regression estimator were observed to be 5.74 and 4.68 mmHg for the SBP and DBP, respectively. The SDE values for the proposed DBN-DNN based ensemble regression estimator were improved by 4.31 and 3.61 mmHg for the SBP and DBP, respectively, as compared with those of the conventional MAA, as shown in Table 6. There were differences of 1.37 and 1.46 mmHg in the SDEs for the SBP and DBP, respectively, between the proposed DBN-DNN based ensemble regression estimator and the SVR model. Additionally, comparing the proposed DBN-DNN based ensemble regression estimator with the DBN-DNN based single regression model, we found that the SDEs of the SBP and DBP were reduced by 0.46 and 0.58 mmHg, respectively. These mean that the proposed method improved the performance by 7.4% and 11 % compared with the DBN-DNN based single regression model.

The results of the FFNN and GMR models are also presented in Table 6. In particular, we utilized the SVR algorithm with a linear epsilon insensitive cost function [33] as the opponent technique in the current state of the art to evaluate the performance of the proposed DBN-DNN based ensemble regression estimator fairly. Indeed, the error of the proposed technique was calculated by $(e_i = \hat{t}_i - t_i)$. Thus, ME and root mean square error (RMSE) were readily defined as $(\frac{1}{n}\sum_{i=1}^{n} e_i)$ and $\sqrt{(\frac{1}{n}\sum_{i=1}^{n} |e_i|^2)}$, respectively. Therefore, the SDEs of the ME and RMSE were easily computed through the statistical method as shown in Table 6.

Moreover, we computed the percentages of the MAEs for three categories, ≤ 5 mmHg, ≤ 10 mmHg, and ≤ 15 mmHg, for all measurements (425 measurements). The protocol of

TABLE 7. Grading of the proposed algorithm based on the BHS standard using the results of MAA, FFNN, SVR [33], GMR, DBN-DNN [19], and DBN-DNN ensemble on (5 × 85 = 425) measurements.

Tests	SBP Absolute difference (%)			DBP Absolute difference (%)			Standard (SBP/DBP) BHS
	≤5 mmHg	≤10 mmHg	≤15 mmHg	≤5 mmHg	≤10 mmHg	≤15 mmHg	Grade
MAA	47.06	85.88	96.47	56.47	88.24	97.65	C/B
FFNN	53.88	85.65	95.53	66.12	94.12	98.82	B/A
SVR	62.59	86.12	95.53	74.12	93.65	96.94	A/A
GMR	67.00	90.00	95.00	63.70	87.76	97.65	A/A
DBN-DNN	69.65	90.12	95.53	76.19	95.76	98.82	A/A
DBN-DNN ensemble	71.06	90.82	95.53	81.18	96.24	99.29	A/A

the BHS with an A-D graded system would grant a grade of A to a device if 60% of its error measurements are within 5 mmHg, 85% of its error measurements are within 10 mmHg, and 95% of its error measurements falls within 15 mmHg [31]. Furthermore, Bland-Altman plots to compare the performance of the proposed DBN-DNN based fusion ensemble model with the auscultatory nurse measurements (425 measurements) are represented in Fig. 5. In addition, the results of the BHS protocol [31] indicate that the DBN-DNN based fusion ensemble regression estimator provided accurate BP estimates when compared to the MAA, FFNN, SVR, GMR, and DBN-DNN based single regression techniques. In Table 7, we also report the BHS grading scores obtained by the DBN-DNN based fusion ensemble regression estimator. The results of the proposed DBN-DNN based fusion ensemble regression estimator were 71.06 % (≤5 mmHg), 90.82 % (≤10 mmHg), and 95.53 % (≤15 mmHg) for the SBP in the given experimental test scenario and 81.18 % (≤5 mmHg), 96.24 % (≤10 mmHg), and 99.29 % (≤15 mmHg) for the DBP in the experimental test scenario.

IV. DISCUSSION AND CONCLUSION

As mentioned in the results section, we found that the proposed DBN-DNN based ensemble regression estimator was superior to the conventional algorithms, as shown in Tables 4, 5, 6 and 7. These mean that sufficient mimic features are an important aspect for improving the generalization capacity of the proposed DBN-DNN based ensemble regression estimator. In consequence, the proposed DBN-DNN based ensemble regression estimator obtains an overall grade of A based on the BHS grading system. Additionally, we also assessed the performance of the DBN-DNN based ensemble regression estimator using regression and Bland-Altman plots as shown in Figs. 4 and 5. These indicate that the BP estimates acquired by the proposed DBN-DNN based ensemble regression estimator are in very close agreement with the reference BPs (SBP and DBP). The bounds of agreement (see bold horizontal lines in Fig. 5) that we used were (ME $\pm$ 2$\times$ SDE) for two plots, the mostly black asterisks lie within the bounds of agreement. The biases (see horizontal center lines) for the two plots were practically small ($\leq \pm$ 0.5 mmHg). In particular, Fig. 5 beautifully demonstrates results in accord with the last column in Table 6. Therefore, based on the results of the overall performance evaluation, we have clearly demonstrated that the proposed DBN-DNN based ensemble regression estimator mitigates the estimation uncertainty and improves the confidence of the proposed technique.

In conclusion, the DBN-DNN based ensemble regression estimator with a small sample obtained lower SDEs and MEs for the SBP and the DBP compared to conventional algorithms. The main contribution of the proposed algorithm is that the accuracy and stability are improved using the DBN-DNN based fusion ensemble regression estimator in a small sample environment based on the bootstrap-inspired technique. We also found the distribution of mimic feature is asymptotical Gaussian that is quite well fit for the proposed ensemble regression estimator as the number of training data increases. Our future study will include clinical testing on a wide range of new subjects based on the ANSI/AAMI SP 10 and BHS protocols. Moreover, since the proposed DBN ensemble is highly time consuming when compared to the single DBN-DNN model, optimization can be further used to simplify the structure and enhance the efficiency of the DBN-DNN based ensemble regression estimator.

REFERENCES

[1] G. Drzewiecki, R. Hood, and H. Apple, "Theory of the oscillometric maximum and the systolic and diastolic detection ratios," *Ann. Biomed. Eng.*, vol. 22, no. 1, pp. 88–96, Jan./Feb. 1994.

[2] L. A. Geddes, M. Voelz, C. Combs, D. Reiner, and C. F. Babbs, "Characterization of the oscillometric method for measuring indirect blood pressure," *Ann. Biomed. Eng.*, vol. 10, no. 6, pp. 271–280, Nov. 1982.

[3] S. Lee, M. Bolic, V. Z. Groza, H. R. Dajani, and S. Rajan, "Confidence interval estimation for oscillometric blood pressure measurements using bootstrap approaches," *IEEE Trans. Instrum. Meas.*, vol. 60, no. 10, pp. 3405–3415, Oct. 2011.

[4] C. F. Babbs, "Oscillometric measurement of systolic and diastolic blood pressures validated in a physiologic mathematical model," *Biomed. Eng. Online*, vol. 11, no. 1, p. 56, Aug. 2012.

[5] K. Soueidan *et al.*, "Augmented blood pressure measurement through the noninvasive estimation of physiological arterial pressure variability," *Physiol. Meas.*, vol. 33, no. 6, pp. 881–899, May 2012.

[6] C. Cuspidi *et al.*, "Prevalence of home blood pressure measurement among selected hypertensive patients: Results of a multicenter survey from six hospital outpatient hypertension clinics in Italy," *Blood Pressure*, vol. 14, no. 4, pp. 251–256, 2014.

[7] *American National Standard Manual, Electronic or Automated Sphygmonanometers*, document AASI/AAMI SP 10:2002, Association for the Advancement of Medical Instrumentation (AAMI), 2003.

[8] S. Hansen and M. Staber, "Oscillometric blood pressure measurement used for calibration of the arterial tonometry method contributes significantly to error," *Eur. J. Anaesthesiol.*, vol. 23, no. 9, pp. 781–787, Sep. 2006.

[9] D. W. Jones and J. E. Hall, "Hypertension: Pathways to success," *Hypertension*, vol. 51, no. 5, pp. 1249–1251, May 2008.

[10] P. D. Baker, J. A. Orr, D. R. Westenskow, and T. P. Egbert, "Method for determining blood pressure utilizing a neural network," U.S. Patent 5 339 818 A, Aug. 23, 1994.
[11] S. Narus, T. Egbert, T.-K. Lee, J. Lu, and D. Westenskow, "Noninvasive blood pressure monitoring from the supraorbital artery using an artificial neural network oscillometric algorithm," *J. Clin. Monitor.*, vol. 11, no. 5, pp. 289–297, Sep. 1995.
[12] D. D. Hickey, "Method and apparatus for measuring blood pressure," U.S. Patent 5 048 532, Sep. 17, 1991.
[13] T. Arai, K. Lee, and R. J. Cohen, "Cardiac output and stroke volume estimation using a hybrid of three Windkessel models," in *Proc. Annu. Int. Conf. IEEE Eng. Med. Biol. Soc.*, Buenos Aires, Argentina, Aug./Sep. 2010, pp. 4971–4974.
[14] M. Forouzanfar, H. R. Dajani, V. Z. Groza, M. Bolic, and S. Rajan, "Feature-based neural network approach for oscillometric blood pressure estimation," *IEEE Trans. Instum. Meas.*, vol. 60, no. 8, pp. 2786–2796, Aug. 2011.
[15] X.-L. Zhang and J. Wu, "Deep belief networks based voice activity detection," *IEEE Trans. Audio, Speech, Language Process.*, vol. 21, no. 4, pp. 697–710, Apr. 2013.
[16] G. E. Hinton, S. Osindero, and Y.-W. Teh, "A fast learning algorithm for deep belief nets," *Neural Comput.*, vol. 18, no. 7, pp. 1527–1554, 2006.
[17] Y. Lei, F. Jia, J. Lin, S. Xing, and S. X. Ding, "An intelligent fault diagnosis method using unsupervised feature learning towards mechanical big data," *IEEE Trans. Ind. Electron.*, vol. 63, no. 5, pp. 3137–3147, May 2016.
[18] M. D. Prieto, G. Cirrincione, A. G. Espinosa, J. A. Ortega, and H. Henao, "Bearing fault detection by a novel condition-monitoring scheme based on statistical-time features and neural networks," *IEEE Trans. Ind. Electron.*, vol. 60, no. 8, pp. 3398–3407, Aug. 2013.
[19] S. Lee and J.-H. Chang, "Oscillometric blood pressure estimation based on deep learning," *IEEE Trans. Ind. Informat.*, vol. 13, no. 2, pp. 461–472, Apr. 2017.
[20] P. Buhlmann and B. Yu, "Analyzing bagging," *Ann. Statist.*, vol. 30, no. 4, pp. 927–961, Aug. 2002.
[21] Y. Freund and R. E. Schapire, "A decision-theoretic generalization of on-line learning and an application to boosting," *J. Comput. Syst. Sci.*, vol. 55, no. 1, pp. 119–139, Aug. 1997.
[22] T. G. Dietterich, "Ensemble methods in machine learning," in *Proc. Multiple Classifier Syst.*, 2000, pp. 1–15.
[23] S. Lee *et al.*, "Oscillometric blood pressure estimation based on maximum amplitude algorithm employing Gaussian mixture regression," *IEEE Trans. Instum. Meas.*, vol. 62, no. 12, pp. 3387–3389, Dec. 2013.
[24] S. Lee, C.-H. Park, and J.-H. Chang "Improved Gaussian mixture regression based on pseudo feature generation using bootstrap in blood pressure estimation," *IEEE Trans. Ind. Informat.*, vol. 12, no. 6, pp. 2269–2280, Dec. 2016.
[25] F. J. Massey, Jr., "The Kolmogorov–Smirnov test for goodness of fit," *J. Amer. Statist. Assoc.*, vol. 46, no. 253, pp. 68–78, 1951.
[26] Y. Bengio, "Learning deep architectures for AI," *Found. Trends Mach. Learn.*, vol. 2, no. 1, pp. 1–127, 2009.
[27] B. Efron, *An Introduction to the Bootstrap*. London, U.K.: Chapman & Hall, 1993.
[28] Y. Xu, J. Du, L. R. Dai, and C. H. Lee, "A regression approach to speech enhancement based on deep neural networks," *IEEE/ACM Trans. Audio, Speech, Language Process.*, vol. 23, no. 1, pp. 7–19, Jan. 2015.
[29] S. Lee, C. Lim, and J.-H. Chang, "A new *a priori* SNR estimator based on multiple linear regression technique for speech enhancement," *Digit. Signal Process.*, vol. 30, no. 7, pp. 154–164, Jul. 2014.
[30] M. R. Neuman, "Measurement of blood pressure," *IEEE Pulse*, vol. 2, no. 2, pp. 39–44, Mar./Apr. 2011.
[31] E. O'Brien *et al.*, "The British hypertension society protocol for the evaluation of blood pressure measuring devices," *J. Hypertens.*, vol. 11, no. 6, pp. 667–679, 1993.
[32] M. Knapp-Cordes and B. McKeeman, "Improvements to tic and toc functions for measuring absolute elapsed time performance in MATLAB," in *MATLAB Technical Articles and Newsletters*. Natick, MA, USA: The MathWorks, 2011.
[33] A. Rakotomamonjy, "Analysis of SVM regression bound for variable ranking," *Neurocomputing*, vol. 70, nos. 7–9, pp. 1489–1501, Mar. 2007.

SOOJEONG LEE received the Ph.D. degree in computer engineering from Kwangwoon University, Seoul, South Korea, in 2008. From 2009 to 2011, he was a Post-Doctoral Fellowship with the School of Information Technology and Engineering, University of Ottawa, Canada. He is currently a Research Professor with the School of Electronic Engineering, Hanyang University, Seoul. His areas of the interest are speech signal processing, noise estimation and reduction, bio-signal processing, instrumentation and measurement, and machine learning.

JOON-HYUK CHANG (SM'09) received the B.S. degree in electronics engineering from Kyungpook National University, Daegu, South Korea, in 1998, and the M.S. and Ph.D. degrees in electrical engineering from Seoul National University, South Korea, in 2000 and 2004, respectively. From 2000 to 2005, he was with Netdus Corp., Seoul, as a Chief Engineer. From 2004 to 2005, he held a post-doctoral position with the University of California at Santa Barbara, Santa Barbara, where he was involved in adaptive signal processing and audio coding. In 2005, he joined the Korea Institute of Science and Technology, Seoul, as a Research Scientist, where he was involved in speech recognition. From 2005 to 2011, he was an Assistant Professor with the school of Electronic Engineering, Inha University, Incheon, South Korea. He is currently a Full Professor with the School of Electronic Engineering, Hanyang University, Seoul, South Korea. His research interests are in speech coding, speech enhancement, speech recognition, audio coding, and adaptive signal processing. He was recipient of the IEEE/IEEK IT Young Engineer of the year 2011. He is serving as an Editor-in-chief of the *Signal Processing Society Journal* of the IEEK.